

AD-A136 144

CHARACTERISTICS OF THE MECHANICAL PROPERTIES AND THE
FRACTURES OF AN ALPH. (U) FOREIGN TECHNOLOGY DIV
WRIGHT-PATTERSON AFB OH G ZHIMING 18 NOV 83

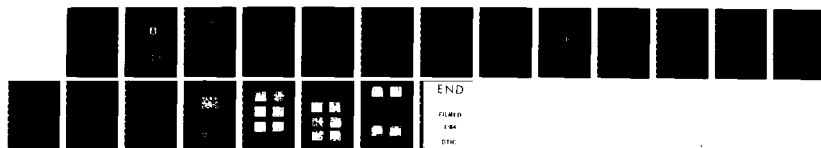
1/1

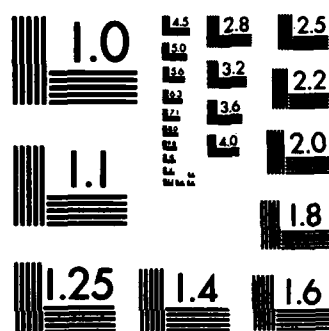
UNCLASSIFIED

FTD-ID(RS)T-1575-83

F/G 11/6

NL





MICROCOPY RESOLUTION TEST CHART
NATIONAL BUREAU OF STANDARDS-1963-A

2

FTD-ID(RS)T-1575-83

AD-A136144

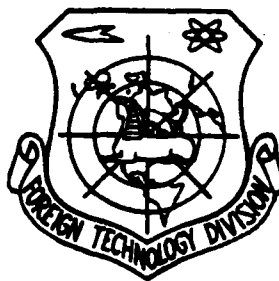
FOREIGN TECHNOLOGY DIVISION



CHARACTERISTICS OF THE MECHANICAL PROPERTIES AND THE FRACTURES
OF AN ALPHA BETA TITANIUM ALLOY

by

Ge Zhiming



DTIC
ELECTE
DEC 19 1983
S E D

Approved for public release;
distribution unlimited.

DTIC FILE COPY



83 12 19 124

EDITED TRANSLATION

FTD-ID(RS)T-1575-83

18 November 1983

MICROFICHE NR: FTD-83-C-001419

CHARACTERISTICS OF THE MECHANICAL PROPERTIES AND
THE FRACTURES OF AN ALPHA BETA TITANIUM ALLOY

By: Ge Zhiming

English pages: 15

Source: ~~Hang Kong~~ Cailiao Yanjiusua, Vol. 1, Nr. 2,
December 1981, pp. 8-14; 5-8

Country of Origin: China

Translated by: SCITRAN

F33657-81-D-0263

Requester: FTD/TQTA

Approved for public release; distribution unlimited.

THIS TRANSLATION IS A RENDITION OF THE ORIGINAL FOREIGN TEXT WITHOUT ANY ANALYTICAL OR EDITORIAL COMMENT. STATEMENTS OR THEORIES ADVOCATED OR IMPLIED ARE THOSE OF THE SOURCE AND DO NOT NECESSARILY REFLECT THE POSITION OR OPINION OF THE FOREIGN TECHNOLOGY DIVISION.

PREPARED BY:

TRANSLATION DIVISION
FOREIGN TECHNOLOGY DIVISION
WP-AFB, OHIO.

FTD-ID(RS)T-1575-83

Date 18 Nov 1983

GRAPHICS DISCLAIMER

All figures, graphics, tables, equations, etc. merged into this translation were extracted from the best quality copy available.

Accession For	
NTIS GRA&I	<input checked="" type="checkbox"/>
DTIC TAB	<input type="checkbox"/>
Unannounced	<input type="checkbox"/>
Justification	
By	
Distribution/	
Availability Codes	
Dist	Avail and/or Special
A-1	



Characteristics of the Mechanical Properties and the Fractures of an Alpha Beta Titanium Alloy

/8

Ge Zhiming

ABSTRACT

This work compared the mechanical properties and the electron fractography of three types of annealed structures of a martensite type α - β titanium alloy (Ti-6.5 Al-3.5 Mo-2 Zr-0.3 Si). These three types of structures were: the equiaxed microstructure (the volume fraction of the primary α structure was around 50%), the mixed structure (a structure with alternately aligned nearly equiaxed α grains and distorted lamellar α structure), and the lamellar structure (the lamellar α + β Widmanstätten structure + the α grain boundary). It was discovered that, in the aspects of tensile, impact, fatigue, and room temperature tensile property after extended exposure to 500°C, the equiaxed structure is superior to the other two structures. However, in the aspects of stress rupture and creep strength, the mixed structure is superior to the other two structures. The mixed structure has better overall characteristics. The characteristic of the electron fractograph of the equiaxed structure and the mixed structure showed a dimple pattern. The fracture characteristic of the lamellar structure was found to be the intergranular fracture type with microvoids.

Although many studies have been carried out to investigate the effect of the characteristics of the two typical microstructures (the equiaxed structure and the lamellar structure) of the α - β titanium alloy, as well as the variation of the structural parameters, on the properties of the alloy (1-8), yet the study of some boundary structures with practical values, such as the "dual status structure" whose primary equiaxed α structure volume fraction is 10-30% and the "mixed structure" obtained through distortion around the transformation point of $(\alpha + \beta)/\beta$, is still not enough.

The purpose of this paper was to study the characteristic features and the fractures of the typical annealed structures of

the α - β titanium alloy and to explore the feasibility of using the mixed structure in practice through a comparative analysis of the mechanical properties and fractographs of the three types of microstructures (the equiaxed structure, the mixed structure, and the lamellar structure) of the Ti-6.5 Al-3.5 Mo-2 Zr-0.3 Si alloy.

MATERIALS AND EXPERIMENTAL METHODS

After considering the prospect in practical applications, the thermally strengthened martensitic Ti-6.5 Al-3.5 Mo-2 Zr-0.3 Si α - β titanium alloy was chosen in this work. The composition of the experimentally used alloy was analyzed and the results are as follows: 6.38% Al, 3.45% Mo, 1.99% Zr, 0.32% Si, 0.072% Fe, 0.01% C, 0.10% O, 0.0065% N, and 0.008% H.

The three different types of microstructures were prepared on the rod materials used in the experiments by the following methods: the I type equiaxed structure adopted the low temperature $\alpha + \beta$ rolling method; the II type mixed structure used the β zone heating continuous rolling method, and distortion was completed in the $\alpha + \beta$ region; and the III type lamellar structure adopted the β treatment. The rod materials with three types of structures were doubly annealed (950°C/1 hour/air cooling + 530°C/6 hours/air cooling).

Properties such as the tensile characteristics, room temperature impact, room temperature fatigue characteristics with smooth and notched materials, rupture resistance and creep at 500°C, and long term thermal stability at 500°C without stress were determined comparatively using rod materials with the three types of microstructures at various temperatures. Their microstructures and scanning electron fractographs were analyzed and observed.

EXPERIMENTAL RESULTS

1. The Microstructure

The typical microstructures of the three types are shown in Figure 1 (see Plate 5). The volume fraction of the equiaxed primary α structure in the Type I structure is usually about 50%. The average diameter of the recrystallized β grain is approximately 4-8 micron. The size of an equiaxed primary α grain is usually on the same order of magnitude as the grain size of a recrystallized β grain.

There are two α states in the Type II structure. One is nearly an equiaxed α grain. Their predecessors have the lamellar α structure which are first nucleated and grown in the primary β grain boundary and in the grain. It is formed because it was fully crushed in the $\alpha + \beta$ region due to a large distortion. The other type is a distorted lamellar α structure whose aspect ratio is usually less than 10:1. Their predecessors have the straight lamellar α structure which are nucleated and grown late in the primary β grains. Because of the relatively small distortion in the $\alpha + \beta$ region, they are not crushed sufficiently. In this mixed structure which consists of an alternatively arranged nearly equiaxed α grains and distorted lamellar α structure, it is not possible to see the clear primary β grains and α grain boundaries. However, the trace of the original α groups can still be observed. Its dimension is usually around 20-30 microns.

The characteristic of the Type III structure is that the β grain surrounded by the α grain boundary is very thick. The diameter of the grain is usually in the range of 200-800 microns. The average is around 400 microns. The lamellar α structure in the grain is thin, flat, and long.

2. Mechanical Characteristics

The comparison of the tensile properties of the rod materials with three types of microstructures at various temperatures is shown in Figure 2. Within the temperature range from room temperature to 500°C, regardless whether it is the tensile strength or plasticity, Type I structure has the highest value. Type II is situated in the middle. Type III is the lowest. Especially in terms of the contraction ratio of fracture, the Type III structure differs by 20-30% from Types I and II structures.

The comparison of the room temperature rotational bending fatigue limits for smooth and notched ($K_t = 1.9$) specimens* are shown in Figures 3 and 4, respectively. In all cases, the Type I structure is the highest. Type II is in the middle, and Type III is the lowest.

The difference in the impact toughness of the three types of microstructures is also relatively obvious, i.e. the room temperature impact value of the Type I structure is the highest

* 2×10^7 basic cycles

which reaches $5.7 \text{ Kg}\cdot\text{m}/\text{cm}^2$. The Type II structure is next, which is $4.6 \text{ Kg}\cdot\text{m}/\text{cm}^2$. The Type III structure is the lowest, only $3.2 \text{ Kg}\cdot\text{m}/\text{cm}^2$.

The relation between the measured room temperature tensile properties and the exposure time to heat of tensile specimens of various structures after 100-2000 hours of exposure to 500°C without any stress are shown in Figure 5. From the figure, one can see that with increasing heat exposure time, the room temperature tensile strength increases in specimens of various types of structures. However, they still maintain the same differences among them as those before the thermal exposure.

If the relative reductions in ductility and fracture contraction ratio after and before the thermal exposure (expressed in terms of ratios such as δ/δ_0 and ψ/ψ_0) are used as the gauge to judge the thermal stability of the alloy, then one can see from Figure 5 that the thermal stability of this alloy is the best in the Type I structure, Type II structure is next, and Type III structure is the worst.

The comparison of the stress-rupture limit and the creep limit measured with smooth and notched ($K_t = 2.3$) specimens at 500°C in three types of structures is shown in Figure 6. From the figure, one can see that the stress-rupture limit and creep limit at 500°C are the highest with the Type II structure regardless of the fact whether smooth or notched specimens were used. The next is the Type III structure. The Type I structure is the lowest.

Figure 2. Comparison of Tensile Characteristics of Rod Materials in Three Different Types of Structures at Various Temperatures.

/10

1. Type I Structure.
2. Type II Structure.
3. Type III Structure.
4. Temperature, $^\circ\text{C}$.

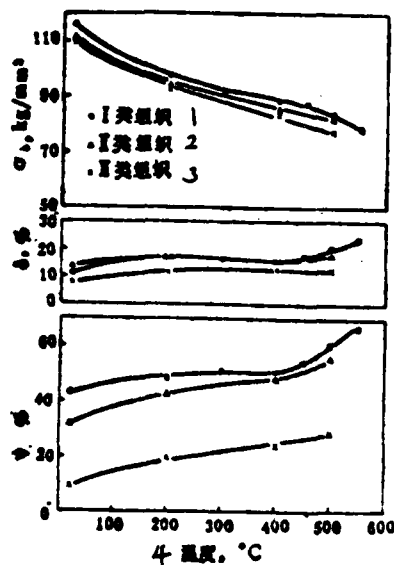


Figure 3. Comparison of the Room Temperature Smooth Fatigue Limit of Rod Materials with Three Different Types of Structures.



Figure 4. Comparison of the Room Temperature Notched Fatigue Limit of Rod Materials with Three Different Types of Structures.

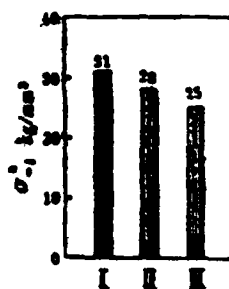


Figure 5. Comparison of the Tensile Characteristics Before and After the Prolonged Thermal Exposure at 500°C Without Stress for Specimens With Three Types of Structures: δ_0 , δ , ψ_0 , ψ - Represent the Ductility and Fracture Contraction Ratio Before and After the Heat Exposure, Respectively.

1. Type I Structure.
2. Type II Structure.
3. Type III Structure.
4. Time, hour.

*The alloy used to prepare the Type I structure specimen was another brand. Its' tensile strength is approximately 10 Kg/mm² lower than that of the brand of alloy used in this research institute. Therefore, the tensile strength of the Type I structure in the figure above is lower than those of the Type II & III structures.

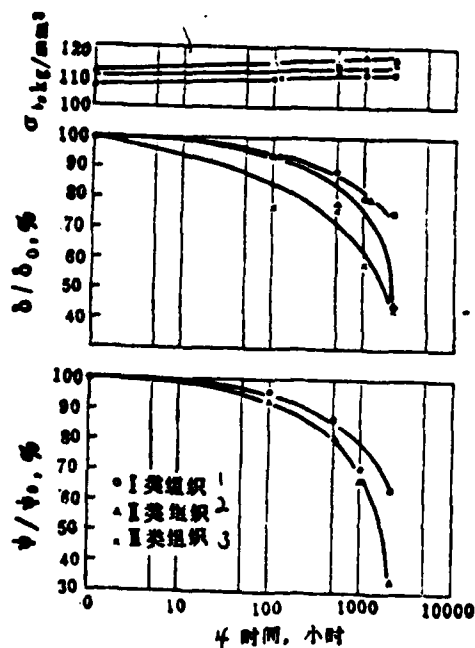
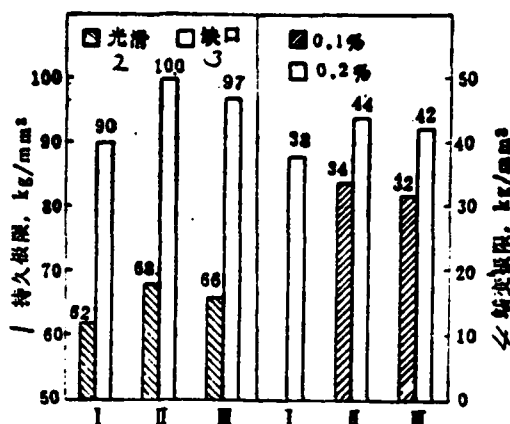


Figure 6. Comparison of the Stress Rupture Limit and the Creep Limit of Rod Materials in Three Types of Structures at 500°C.

1. Stress Rupture Limit, Kg/mm².
2. Smooth.
3. Notched.
4. Creep Limit, Kg/mm².



3. Fracture Characteristics

/11

Scanning electron fractographic observation shows that the characteristics of the electron fractographs of the tensile, impact and 500°C sustaining specimens in Types I and II structures have the dimple fracture pattern. The dimples on the fracture of the Type I structure room temperature tensile specimen are relatively fine and evenly distributed. Its' dimension is approximately equivalent to the grain size of the equiaxed α grain and the recrystallized β grain in the microstructure (Figure 7a, see Plate 6, Figure 1a). The dimension of the dimples of the Type II tensile fracture also almost corresponds to the size of the α grain or α lamellar structure in the microstructure (Figure 7b, see plate 6, Figure 1b). The dimples on the electron fractographs of the 500°C stress rupture specimens with the Types I and II structures are relatively large. Moreover, a lot of secondary cracks appeared. On the fearing line between the large dimples, one can see a series of small dimples in a string (see Figures 7c and d in Plate 6).

The characteristics of the electron fractographic specimens used in tensile, impact, and 500°C endurance tests in the Type III structure showed the intergranular fracture of the microvoid coalescence type. One can see the "rock shaped" β grain morphology in the fractograph of a relatively low magnificational (Figure 7e, see Plate 6). In a fractograph at a high magnification, one can

see the secondary cracks, which propagate along the grain boundary and dimples. The dimension and distribution of the latter are closely related to the intragranular structure of the β grain particles (Figures 7f, g, h, see Plates 6, 7).

The electron fractographs of the fractures of fatigue specimens in different structures are shown in Figure 8 (see Plates 7 and 8). From the figure, one can see that the fatigue fracture characteristics of the Types I and II structures are very similar. In the fatigue crack propagating region, it is possible to see fine fatigue belts and a certain number of secondary cracks (Figures 8a, c). The electron fractograph of the instantaneously fractured region is characteristic by the dimples (Figures 8b,d). The fatigue fracture characteristics of the Type III structure are wider fatigue belts and more secondary cracks. A brittle fatigue belt emerges in the front section of the crack propagation zone (Figure 8e). In the rear section of the crack propagation zone, it is possible to see the plastic fatigue belt (see Figure 8f). The instantaneous fracture zone is characterized by the intergranular fracture of the microvoid coalescence type (Figures 8g, h).

DISCUSSION

Margolin and Greenfield pointed out in their study on the tensile fracture mechanism of the α - β titanium alloys that the fracture stress is inversely proportional to the distance between the equiaxed primary α grains and the square root of the diameter of the prior β grain for an equiaxed structure. For a lamellar structure, its fracture stress is inversely proportional to the diameter of the β grain and the thickness of the α grain boundary (9). Furthermore, for a given annealing temperature, the average diameter of the equiaxed α structure in an equiaxed structure is proportional to the diameter of the prior β grain (10). Therefore, the fracture stress of an equiaxed structure in fact is inversely proportional to the size of equiaxed α grain and the square root of their distance.

The experimental results of this work are that the tensile strength of the fine equiaxed structure of recrystallized β grains

is the highest, and the tensile strength of the lamellar structure of the thick recrystallized β grains is the lowest. The recrystallized β grain size of the mixed structure is in the middle, and its tensile strength is also in the middle (Figure 2). This is in agreement with the result of the study carried out by Margolin, et al. Here, the recrystallized β grain size given by us is the dimension of the α group in the prior sub β grain in the mixed structure. In fact, it is consistent with the distance between the equiaxed α grains in an equiaxed structure because in these structures the prior equiaxed α grains are usually distributed along the grain boundaries of recrystallized β grains (Figure 1a).

In addition to explaining the differences in the aspect of tensile plasticity among the three types of structures by the size of the recrystallized β grain, the α lamellar structure with a continuous grain boundary of a certain thickness also provides a short cut to the nuclear formation and growth of microvoids to a critical size. Consequently, it leads to an intergranular fracture to cause the plasticity of the lamellar structure to be greatly lower than those of the equiaxed and mixed structure.

In titanium alloys, on one hand an equiaxed structure has an even higher resistance against the nuclear formation of fatigue crack as compared to a lamellar structure. However, on the other hand, the crack propagating rate in a lamellar structure is lower than that in an equiaxed structure. But, because of the low stress high cycle number condition, the lifetime consumed in the crack nuclear formation and crack propagation in Stage I is usually over 90% of the total fatigue lifetime (11,12). Therefore, in summary, an equiaxed structure has a relatively longer fatigue lifetime and higher fatigue strength than a lamellar structure. Our experimental results coincided with this pattern, i.e. an equiaxed structure has a much higher fatigue strength than a lamellar structure. The fatigue strength of a mixed structure is located in between those of an equiaxed structure and a lamellar structure. Such a characteristic state of the mixed structure is correlated to the structural characteristics. In the meantime, the difference in the grain

/12

size of the recrystallized β grains of the three types of structures may be one of the reasons why the fatigue strength is quite different (12).

Solonina and Glazunov believed that the room temperature smooth fatigue limit of any heat strengthened titanium alloy to be used in aeronautical engine parts should not be lower than 45% of its tensile strength (13). This is expressed as the horizontal dotted line in Figure 3. From the figure one can see that, among the three types of structures, the equiaxed structure completely satisfies this requirement. The mixed structure is close to this requirement. The lamellar structure, however, is at a considerable distance away from this requirement.

The pattern of variation of the alloy, in terms of its 500°C endurance and creep strength, with the microstructure is opposite to that in the case of room temperature tensile and fatigue strength. Among the three types of structures, the mixed structure is the highest. The lamellar structure is next. The equiaxed structure is the lowest (Figure 6). This is because among the influencing factors affecting the high temperature long term characteristics the sliding of the grain boundary has an important effect. The thickening of the grain, however, can reduce the unfavorable effect of the grain boundary. This is the reason why the creep strength of a thick β grain lamellar structure is usually higher than that of a fine grain size equiaxed structure. In the meantime, in the mixed structure, because the prior β subgrain α group does not exist on a continuous grain boundary, the unfavorable effect of the sliding of the grain boundary is further limited. Therefore, its creep strength and endurance strength are even higher than those of the thick grain lamellar structure.

The results of the study of the scanning electron fractographs showed that the size and distribution of the dimples are closely related to the microstructure in the electron fractographs of equiaxed structure and mixed structure specimens. In the electron fractographs, the distribution of fine and uniform dimples corresponds to the uniform distribution of fine α grains in the transformed β structure. This result of observation is

in agreement with the mechanism of nuclear formation and growth of voids in an equiaxed structure as proposed by Margolin and Greenfield (9).

With regard to a lamellar structure with a continuous α grain boundary, an electron fractographic study proved that it belongs to the intergranular fracture of the microvoid coalescence type. Furthermore, from the viewpoint of the corresponding correlation between the dimple distribution and the morphology of the microstructure in the grain in the electron fractographs (Figure 1c, Figures 7f-h), one can determine that the crack is propagating along the interface between the α grain boundary and the intra-grain structure. This also coincided with the results of studies carried out earlier (9). Moreover, it corresponds to the low tensile plasticity (Figure 2).

In the areas of room temperature tensile, fatigue, impact toughness, thermal stability, fracture characteristics, etc., a mixed structure is relatively similar to an equiaxed structure. However, its high temperature long term characteristics (creep strength and endurance strength) are more superior to those of the other two types of structures. In the meantime, because the nearly equiaxed α grains and the distorted lamellar α structure are arranged alternatively, the resistance against the propagation of cracks would be higher than that of an equiaxed structure. This feature projects that a mixed structure would be more superior to an equiaxed structure in the area of fracture toughness. Therefore, it can be considered that a mixed structure has relatively better overall characteristics among the three types of structures.

From the viewpoint of the heat treatment technology, it is much easier to obtain a mixed structure than an equiaxed structure. It only requires the heating at 10-30°C above the $(\alpha + \beta)/\beta$ transformation point. Distortion takes place first in the β zone and then in the $\alpha + \beta$ zone. Thus the distortion in the β zone can have an effect to further refining the β grains. However, the distortion in the upper $\alpha + \beta$ zone may cause crushed α grain boundaries, and crushed and distorted lamellar α structures.

Once again, through the proper heat treatment, it is possible to obtain a mixed structure with excellent overall characteristics. Therefore, the mixed structure may be used in the actual production of cast parts.

CONCLUSIONS

1. A comparative study on the typical equiaxed structure, lamellar structure, and a borderline structure (i.e. mixed structure) of the α - β titanium alloy Ti-6.5 Al-3.5 Mo-2 Zr-0.3 Si showed that a mixed structure has better comprehensive characteristics. In terms of tensile characteristics, impact toughness, fatigue properties, and heat stability, it is superior to the lamellar structure. However, in the aspects of high temperature creep and endurance strength, it is not only higher than an equiaxed structure, but also higher than a lamellar structure.

2. The electron fractographic characteristic of the equiaxed and mixed structures of this α - β titanium alloy is the dimples. It shows the feature of a toughness fracture. However, the fracture characteristic of a lamellar structure is a microvoid coalescence type intergranular fracture. It has the dual characteristics of the macroscopic embrittlement fracture and microscopic toughness fracture.

3. The mixed structure is worthwhile to be seriously considered as a structure to be used in actual practice. Further study is required.

/13

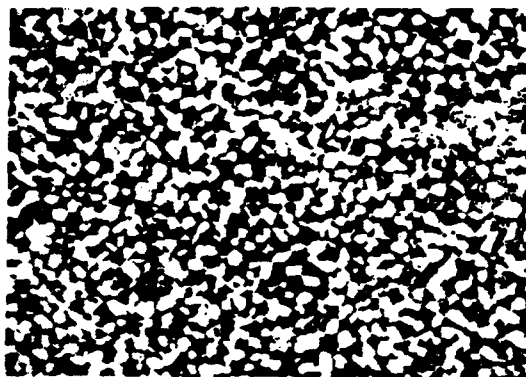
REFERENCES

- [1] Greenfield, M.A., Margolin, H., Met. Trans., 2(1971), No.3, 841.
- [2] Hall, J.A., AD751530, AFML-TR-71-206, Nov. 1971.
- [3] Greenfield, M.A., and others, Titanium Science and Technology, 3(1971), 1731.
- [4] Chesnutt, J. C., and others, AD A063404, AFML-TR-78-68, May 1978.
- [5] Брун, М.Я., Металлведение и термическая Обработка Литейных, 1979, No. 11, 55.
- [6] Achton, S.I., Chambers, L.H., The Science, Technology and Application of Titanium 1970, 879, Pergamon Press, London.
- [7] Peters, M., Extended Abstracts of Fourth International Conference on Titanium, May 1980.
- [8] Thomas, B. and others, AD-A025479, AFML-TR-75-211, Dec. 1975.
- [9] Margolin, H., Greenfield, M. A., Met., Trans., 3(1972), No. 10, 2649.
- [10] Margolin, H. and others, Met. Trans., 4(1973), No. 11, 2519.
- [11] Mahajan, Y. and others, Extended Abstract of Fourth International Conference on Titanium, May 1980.
- [12] Yan Mingao, Aeronautical Materials, 1978, No. 5, 1
- [13] Соломина, О.П., Глазунов, С.Г., Жаропрочные титановые сплавы, (1976), Москва.

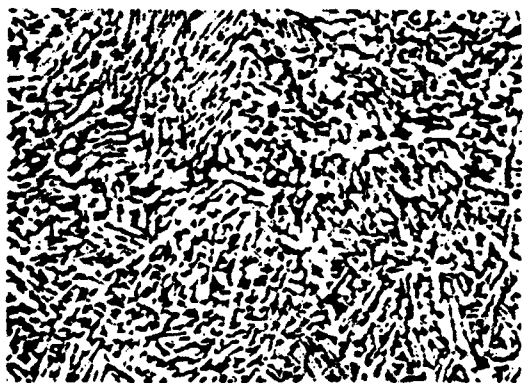
PLATE 5

Figure 1. The Three Annealed Structures of the
Ti-6.5Al-3.5Mo-2Zr-0.3Si Alloy (500X).

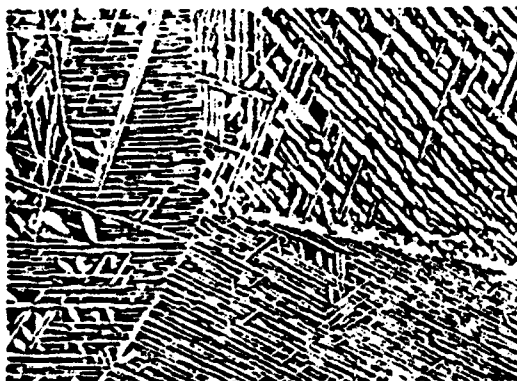
- a. Type I Structure.
- b. Type II Structure.
- c. Type III Structure.



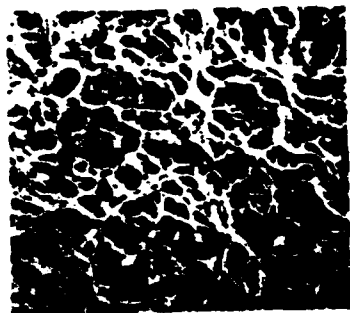
a



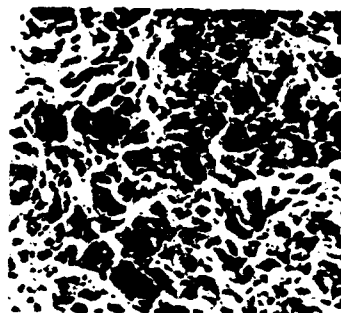
b



c



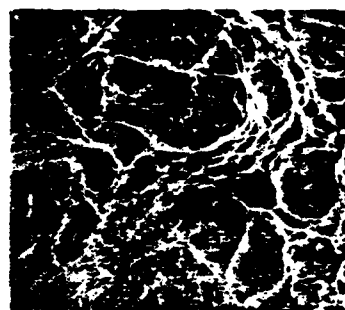
a



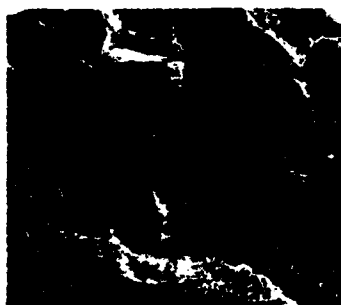
b



c



d



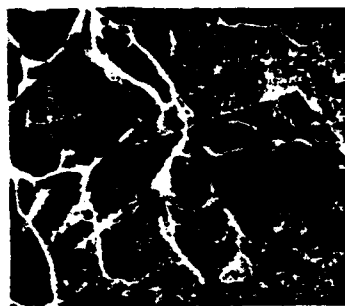
e



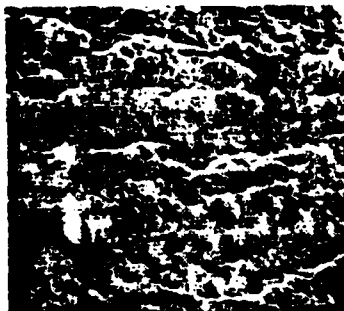
f

Figure 7. The Scanning Electron Fractographs of the Tensile, Endurance, and Impact Fractures of the Three Types of Structures.

- a. Type I Structure, Tensile Fracture, (600X);
- b. Type II Structure, Tensile Fracture, (600X);
- c. Type I Structure, Endurance Specimen, (600X);
- d. Type II Structure, Endurance Specimen, (600X);
- e. Type III Structure, Impact Fracture, Radiation Zone, 30X;
- f. Type III Structure, Impact Fracture, Radiation Zone, 300X;
- g, h. Same as f. (1200X).



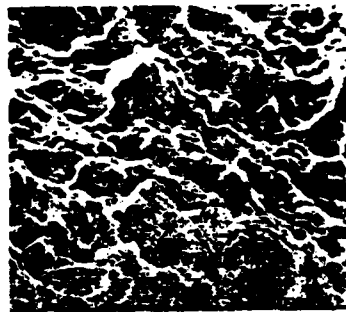
g



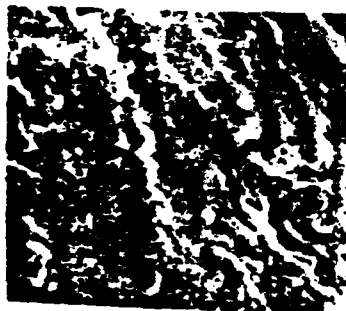
h



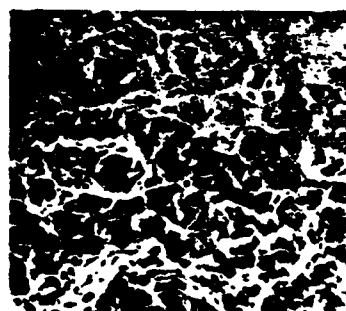
a



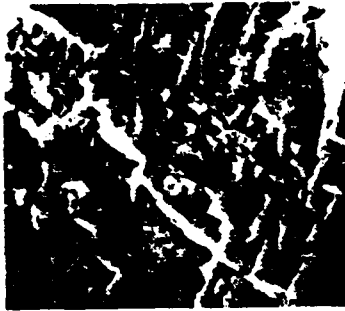
b



c



d



e



f

PLATE 8

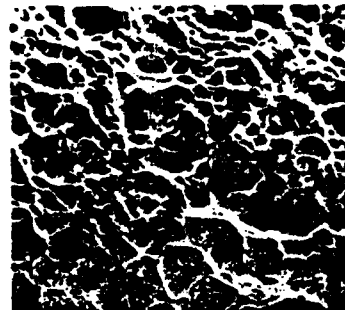
/18

Figure 8. The Scanning Electron Fractographs of the Fatigue Fractures of the Three Types.

- a. Type I Structure, Crack Propagation Zone, (1200X);
- b. Type I Structure, Instantaneous Fracture Zone, (600X);
- c. Type II Structure, Crack Propagation Zone, (600X);
- d. Type II Structure, Instantaneous Fracture Zone, (600X);
- e. Type III Structure, Front of the Crack Propagation Zone, (600X);
- f. Type III Structure, Rear of the Crack Propagation Zone, (600X);
- g. Type III Structure, Instantaneous Fracture Zone, (48X);
- h. Type III Structure, Instantaneous Fracture Zone, (600X);



g



h

END

FILMED

1-84

DTIC